Supplemental material to this article can be found at:
http://jpet.aspetjournals.org/content/suppl/2022/09/19/jpet.122.001280.DC2
http://jpet.aspetjournals.org/content/suppl/2022/09/02/jpet.122.001280.DC1

1521-0103/384/1/61–71$35.00 dx.doi.org/10.1124/jpet.122.001280
THE JOURNAL OF PHARMACOLOGY AND EXPERIMENTAL THERAPEUTICS J Pharmacol Exp Ther 384:61–71, January 2023

The Journal of PHARMACOLOGY And Experimental Therapeutics

Special Section on Non-Coding RNAs in Clinical Practice: From Biomarkers to Therapeutic Tools

CircRNA_33702 Promotes Renal Fibrosis by Targeting the miR-29b-3p/WNT1-Inducible Signaling Pathway Protein 1 Pathway

Kai Ai,[1] Lei Yi,[1] Yinhuai Wang, and Yuan Li

Department of Urology, Second Xiangya Hospital, Central South University, Changsha, People's Republic of China

Received April 20, 2022; accepted August 4, 2022

ABSTRACT

Growing evidence suggest that circular RNAs (circRNAs) are critical mediators in renal diseases. However, there have been very few reports about the role of circRNAs in renal fibrosis. In this study, circRNA_33702 was found to be upregulated, both in unilateral ureteral obstruction (UUO) mice and in TGF-β1–treated Boston University mouse proximal tubule cells. Furthermore, hsa_circ_0026331, homologous with mmu_circ_33702, was found to be upregulated in TGF-β1–treated HK-2 cells. Although knockdown of circRNA_33702 or hsa_circ_0026331 was shown to relieve the TGF-β1–induced expression of collagen I, collagen III, and fibronectin, overexpression of circRNA_33702 was found to exert an inhibitory effect on the expression of the same genes. Mechanistically, circRNA_33702 was demonstrated to bind directly with miR-29b-3p and inhibit its expression. MiR-29b-3p mimic was shown to inhibit the TGF-β1–induced expression of collagen I, collagen III, and fibronectin. Moreover, WNT1-inducible signaling pathway protein 1 (WISP1) was identified as a target of miR-29b-3p, and the expression of WISP1 was observed to be repressed by miR-29b-3p. Notably, knockdown of circRNA_33702 was found to attenuate the expression of collagen I, collagen III, and fibronectin by inhibiting the expression of WISP1, and the observed inhibitory effect can be reversed by miR-29b-3p inhibitor. Finally, inhibition of circRNA_33702 was shown to attenuate interstitial fibrosis in UUO mice via the miR-29b-3p/WISP1 axis. In general, our data show that circRNA_33702 may promote renal fibrosis via the miR-29b-3p/WISP1 axis, which may potentially be developed as a new therapeutic target.

SIGNIFICANCE STATEMENT

This study's findings suggested that circRNA_33702 plays a profibrosis role and that circRNA_33702 with the homologous human hsa_circ_0026331 may be a novel therapeutic target of renal fibrosis.

Introduction

As the final pathway for all chronic kidney diseases, renal tubulointerstitial fibrosis (TIF) can lead to renal failure resulting from the deposition of extracellular matrix (ECM) and from tubular cell loss (Zeisberg and Neilson, 2010; Eddy, 2014; Qi and Yang, 2018). Renal fibrogenesis involves most kidney cell types, with tubular epithelial cell being the key target in a variety of kidney injuries (Liu, 2011; Qi and Yang, 2018). The pathogenesis of TIF involves multiple molecules, such as TGF-β1, which has been widely accepted to play a key role in TIF, and WNT1-inducible signaling pathway protein 1 (WISP1), which has been suggested as a mediator of TGF-β1–induced renal fibrosis in tubular epithelial cells (Böttinger and Bitzer, 2002; Zhong et al., 2017; Chen et al., 2019; Yang et al., 2020b). However, the pathogenetic mechanism of TIF induced by the TGF-β1/WISP1 pathway remains unclear.

Circular RNAs (circRNAs), a novel class of noncoding RNA, is stable against exoribonuclease due to its closed continuous loop that is covalently linked (Guo et al., 2014). CircRNAs play important roles in transcription and protein translation. The main function of circRNAs is to cushion microRNAs (miRNAs),

This study was supported by National Natural Science Foundation of China (81874094 and 82172878) and Natural Science Foundation of Hunan Province of China (2021JJ40818).
The authors confirm that there are no conflicts of interest.
[1]K.A. and L.Y. contributed equally to this work as first authors.
A preprint of this article was deposited in bioRxiv [https://doi.org/10.1101/2022.02.28.482440].
dx.doi.org/10.1124/jpet.122.001280.
S This article has supplemental material available at jpet.aspetjournals.org.

ABBREVIATIONS: BUMPT, Boston University mouse proximal tubule; circRNA, circular RNA; ECM, extracellular matrix; GAPDH, glyceraldehyde-3-phosphate dehydrogenase; Luc, luciferase; miRNA, microRNA; MUT, mutated; qPCR, quantitative PCR; siRNA, small interfering RNA; TFI, tubulointerstitial fibrosis; UUO, unilateral ureteral obstruction; WISP1, WNT1-inducible signaling pathway protein 1.

which means that circRNAs can interfere with miRNAs and their target genes that participate in the progression of various diseases (Zhong et al., 2018). There have been a number of studies that demonstrate circRNAs as important regulators in multiple diseases, especially in cancers (Haque and Harries, 2017; Song and Li, 2018; Zhou et al., 2018). Many recent studies have focused on the link between circRNAs and several renal diseases like acute renal injury, chronic nephritis, and diabetic nephropathy (Luan et al., 2018; Hu et al., 2019).

However, the function of circRNAs on renal fibrosis remains largely unknown. In this study, we found that mmu_circ_33702 was upregulated in both unilateral ureteral obstruction (UUO) mice and in TGF-β1–treated Boston University mouse proximal tubule (BUMPT) cells. Furthermore, hsa_circ_0026331 was upregulated in TGF-β1–treated HK-2 cells (human proximal tubular epithelial cells). We then explored the effect of circRNA_33702 with the homologous hsa_circ_0026331 in renal tubular epithelial cells. Moreover, the downstream target of circRNA_33702 and the underlying mechanism of circRNA_33702 in renal fibrosis were further investigated. Our results may facilitate the development of a novel therapeutic target for renal fibrosis.

Materials and Methods

Antibodies and Reagents. Anti-collagen I, anti-collagen III, anti-fibronectin, and anti-WISP1 antibodies were obtained from Abcam (Cambridge Science Park, Cambridge, UK), whereas anti–glyceraldehyde-3-phosphate dehydrogenase (GAPDH) antibody was purchased from Proteintech North America (Rosemont, IL). Luciferase Assay kit was obtained from BioVision (Milpitas, CA).

Cell Culture and Treatments. BUMPT cells were cultured in high-glucose Dulbecco's modified Eagle's medium (Thermo Fisher Scientific) supplemented with 10% FBS and penicillin-streptomycin (100 U/ml and 100 μg/ml, respectively) at 37°C with CO_2. The cells were transfected with miR-29b-3p inhibitor (100 nM, Ruibo, Guangzhou, China), miR-29b-3p mimic (100 nM), circRNA_33702 small interfering RNA (siRNA) (100 nM), circRNA_33702 plasmid, WISP1 siRNA (100 nM), or negative control (Ruibo, Guangzhou, China) using Lipofectamine 2000 (Life Technologies, Carlsbad, CA). Twenty-four hours after transfection, the cells were treated with serum-free medium overnight, followed by treatment with saline or TGF-β1 (5 ng/ml) for 24 hours. Three circRNA_33702 siRNAs were used, and the most effective target sequence was 5′-TTGTTGATGTTCTGAACCT-3′. The most effective target sequence of WISP1 was 5′-CCACTAGAGGAAACGACTA-3′. HK-2 cells were cultured in Dulbecco's modified Eagle's medium (Sigma-Aldrich, St. Louis, MO) supplemented with 10% FBS and penicillin-streptomycin.

Luciferase Reporter Assays. Luciferase (Luc) vector constructs containing full-length circRNA_33702 [wild-type (WT)-Luc-circRNA_33702], WISP1 3′ UTR (WT-Luc-WISP1), circRNA_33702 fragment that interacts with miR-29b-3p, WISP1 fragment that interacts with miR-29b-3p, mutated (MUT) full-length circRNA_33702 lacking the miR-29b-3p–interacting fragment (MUT-Luc-circ_33702), and mutated WISP1 3′ UTR lacking the miR-29b-3p–interacting fragment (MUT-Luc-WISP1), respectively, were used in this study. Specific target activity was calculated based on the relative luciferase activity ratio of firefly to *Renilla*. All plasmids were obtained from Vigene Biosciences (Jinan, shangdong, China).

BUMPT cells were cotransfected with WT-Luc-circRNA_33702 or MUT-Luc-circRNA_33702, with or without miR-29b-3p mimics. A luciferase reporter assay was performed after incubation for 48 hours as

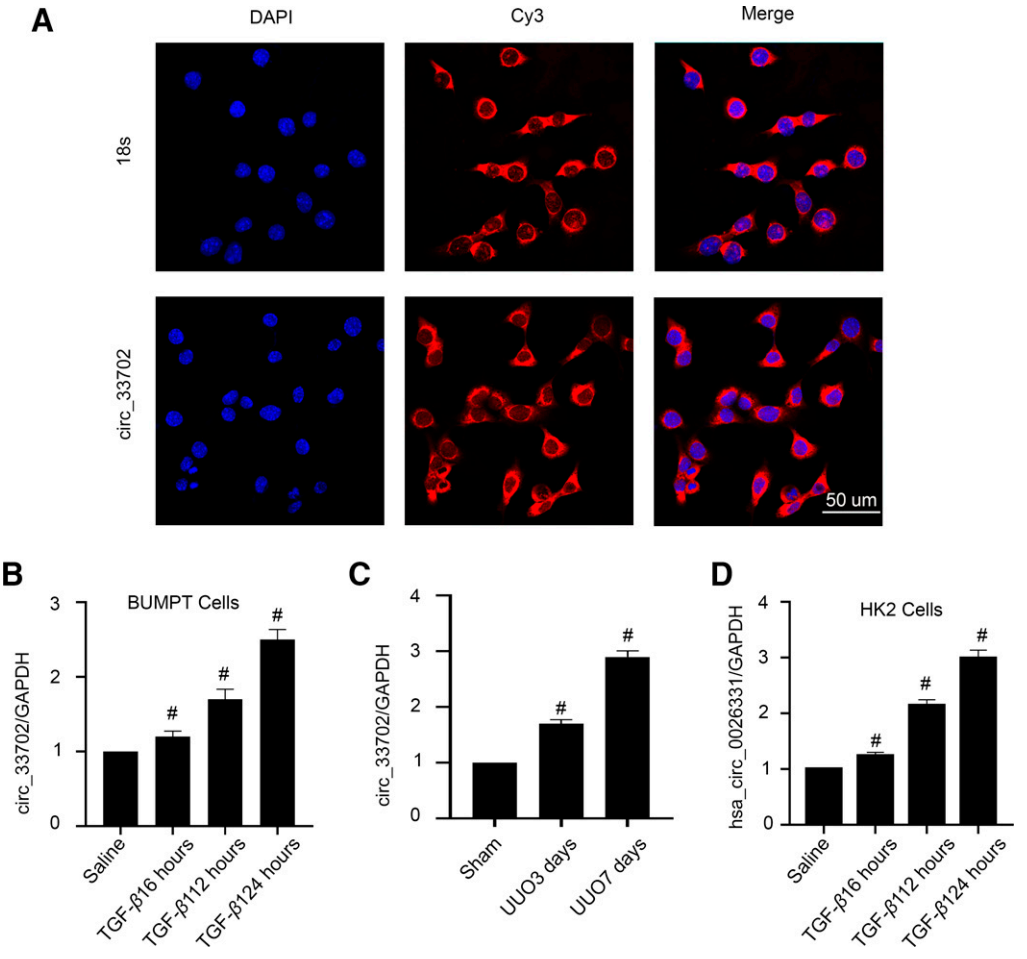

Fig. 1. CircRNA_33702 was induced both in TGF-β1–treated BUMPT cells and in UUO mouse kidneys, and the homologous hsa_circ_0026331 was induced in TGF-β1–treated HK-2 cells. Male C57BL/6 mice were treated with UUO for 0–7 days, and BUMPT cells were treated with 5 ng/ml TGF-β1 for 0–24 hours. (A) Intracellular localization of circRNA_33702 in BUMPT cells. Scale bar, 50 μm. (B and C) Real-time qPCR analyses of circRNA_33702 expression in TGF-β1–treated BUMPT cells and in UUO mouse kidneys. (D) Real-time qPCR analyses of hsa_circ_0026331 expression in TGF-β1–treated HK-2 cells. Data are expressed as mean plus or minus S.D. ($n = 6$). #$P < 0.05$ versus saline or sham group.

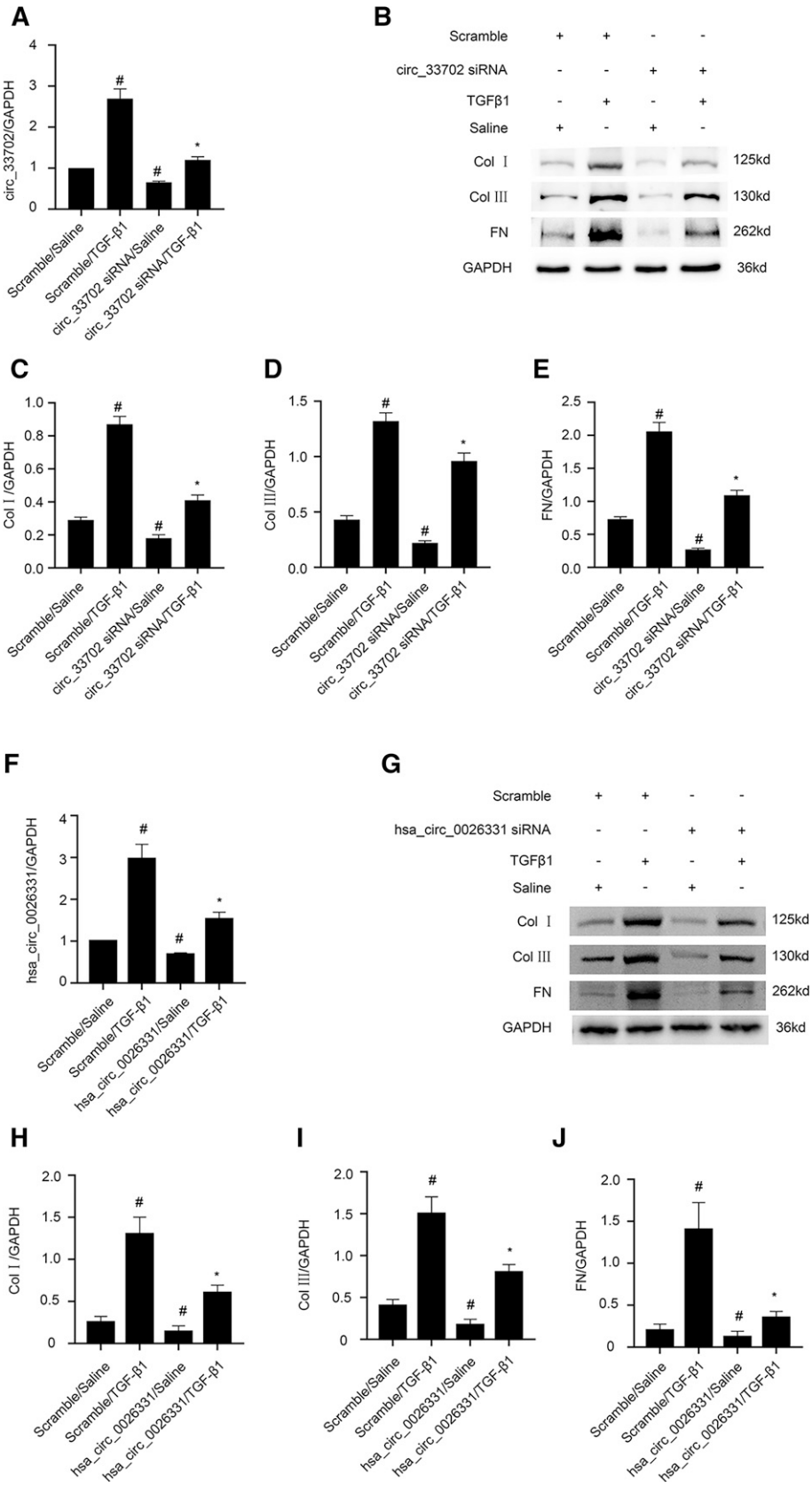

Fig. 2. Inhibition of circRNA_33702 or the homologous hsa_circ_0026331 relieved the TGF-β1–induced expression of collagen I, collagen III, and fibronectin. BUMPT cells were transfected with 50 nM circRNA_33702 or scrambled siRNA before being treated with TGF-β1 or saline for 24 hours. (A and F) Expression of circRNA_33702 (A) and hsa_circ_0026331 (F) detected by real-time qPCR. (B and G) Protein expression of collagen I, collagen III, and fibronectin detected by western blotting. (C–E and H–J) Densitometric measurement of western blot bands for collagen I (C and H), collagen III (D and I), and fibronectin (E and J). Data are expressed as mean plus or minus S.D. (n = 6). #$P < 0.05$ versus control group. *$P < 0.05$, versus TGF-β1 group.

previously described (Kong et al., 2019; Cui and Zhang, 2020; Yang et al., 2020a). Finally, firefly and *Renilla* luciferase activities were measured using Dual-Glo Luciferase Assay System (Promega, Madison, WI) with SpectraMaxM5 (Molecular Devices, Sunnyvale, CA).

Animal Models. The UUO model was established in C57BL/6 mice (male, aged 10–12 weeks) as previously described by ligating the

left ureter with an injection of sodium pentobarbital (Chevalier et al., 2009), using sham-operated mice as controls. The mice were injected twice a week with circ_33702 siRNA or saline via tail vein. The siRNA was 5′Chol + 2′OMe modified, and 15 mg/kg was the minimum dose required for effective inhibition. The mice were housed on a 12-hour light/12-hour dark cycle, with free access to food and water. All animal studies were performed according to the institutional guidelines of Committee for the Care and Use of Laboratory Animals of Second Xiangya Hospital, People's Republic of China.

Histology and Immunohistochemistry. The histology of harvested kidney tissues was analyzed using H&E staining. Fibrotic area was assessed by Masson's trichrome staining. Immunohistochemistry analysis was performed using anti-collagen I (1:100 dilution), anti-collagen III (1:100 dilution), and anti-FN (1:100 dilution) antibodies as previously described (Xu et al., 2019). Immunohistochemistry images were analyzed using an Olympus microscope equipped with UV epi-illumination. The area of renal interstitial fibrosis and renal interstitial gross area were analyzed by Image-Pro Plus 6 (Media Cybernetics, Inc), then the percent area of renal interstitial fibrosis versus renal interstitial gross area was calculated.

Real-Time qPCR. Total RNA was isolated from BUMPT cells and mouse kidney tissues using Trizol reagent (Invitrogen, Carlsbad, CA) according to the manufacturer's protocol., Approximately 40 ng of total RNA was used to synthesize cDNAs using M-MLV Reverse Transcriptase (Invitrogen). To quantify the expression levels of circRNA, mRNA, and miRNA, real-time quantitative PCR (qPCR) was performed using Bio-Rad (Hercules, CA) IQ SYBR Green Supermix with Opticon (MJ Research, Waltham, MA) according to the manufacturer's instructions. The nucleotide sequence of miR-29b-3p was retrieved from GenBank database (gen ID: 387223). The nucleotide sequence of circRNA_33702 was listed in Supplemental Information. The sequences of primers used in this study are as follows: 5′-CCAGCTCTTCTGAAGGAAGCACAG-3′ (circRNA_33702 forward), 5′-TGGCTTAAGGTCCTCCTCAGGTTC-3′ (circRNA_33702 reverse), 5′-CGCGTAGCACCATTTGAAATC-3′ (miR-29b-3p forward), 5′-AGTGCAGGGTCCGAGGTAT-3′ (miR-29b-3p reverse), 5′-GGTCTCCTCTGACTTCACA-3′ (GAPDH forward), and 5′-GTGAGGGTCTCTCTCT-TCCT-3′ (GAPDH reverse). The sequences for U6 primers were used as described previously (Wang et al., 2017). Relative expression of target genes normalized against GAPDH or U6 was calculated using the $2^{-\Delta\Delta Ct}$ method.

Western Blot Analysis. Total protein from BUMPT cells and mouse kidney tissues was extracted by cell lysis, followed by centrifugation at 12,000r at 4°C for 15 minutes. The resulting supernatant fraction of protein lysates was mixed with SDS-PAGE sample buffer containing β-Mercaptoethanol (β-ME) before being boiled at 100°C for 5 minutes. An equal amount of protein lysates was separated by SDS-PAGE before being transferred onto polyvinylidene fluoride (PVDF) membrane (Amersham, Buckinghamshire, UK) for 120 minutes at 290 mA (Peng et al., 2015; Yang et al., 2017; Xu et al., 2019). Transferred membranes were subsequently incubated respectively with primary antibodies against collagen I, collagen III, fibronectin, WISP1, and GAPDH overnight at 4°C, followed by incubation with secondary antibody at room temperature for 60 minutes. Enhanced chemiluminescence (ECL) kit (Millipore) was used to display target protein bands.

Fluorescence in Situ Hybridization. The nucleotide sequence of circRNA_33702 and miR-29b-3p was hybridized using fluorescent probes (Ruibo, Guangzhou, China) as previously described (Zhang et al., 2020). Briefly, BUMPT cells and mouse kidney tissues were incubated with fluorescent probes in hybridization buffer overnight at 4°C. After a washing step with standard saline citrate buffer, the cell nuclei were stained with 4',6-diamidino-2-phenylindole (DAPI) and 18S ribosomal RNA (rRNA) was being used as a cytoplasmic control. Cell images were visualized using a laser-scanning confocal microscope.

Statistical Analyses. Statistical analyses were performed using Graphpad Prism 7. Difference between two groups were compared using two-tailed Student's t tests. Difference between multiple groups were compared using one-way ANOVA. Quantitative data were presented as means plus or minus S.D. $P < 0.05$ was considered statistically significant for all statistical comparisons.

Results

The Expression of mmu_circRNA_33702 Was Upregulated in the Progression of Renal Fibrosis. Our previous study has shown significantly upregulated circRNAs in the UUO-induced renal fibrosis model mice kidney tissues at

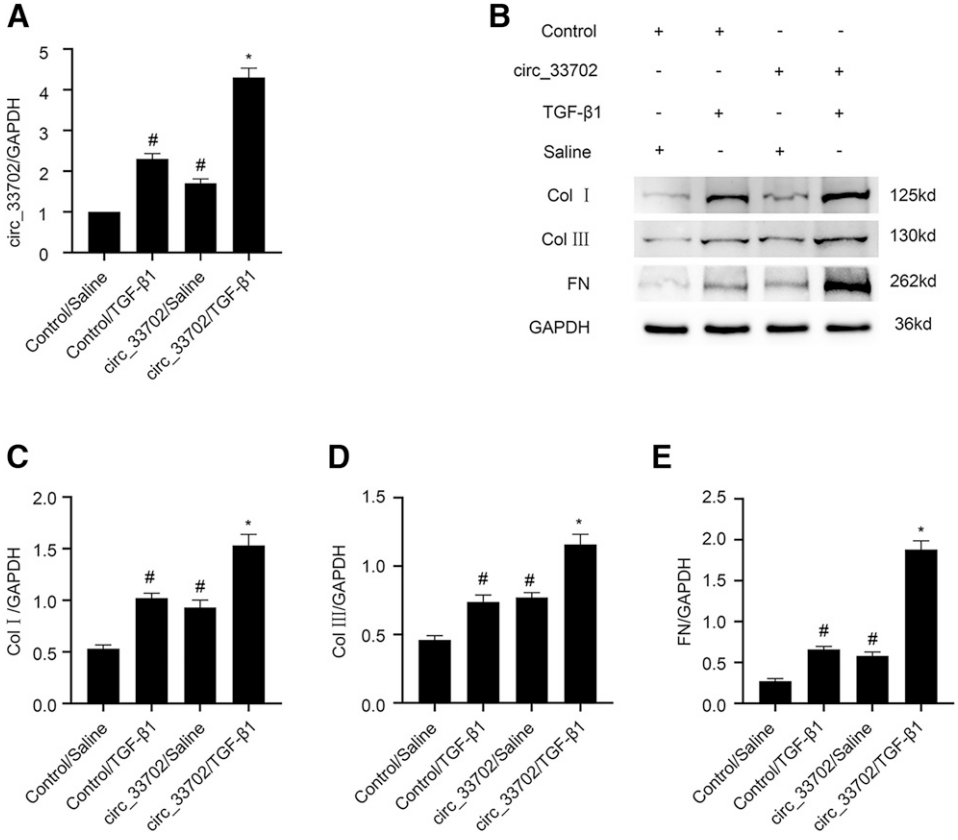

Fig. 3. Overexpression of circRNA_33702 aggravated TGF-β1–induced expression of collagen I, collagen III, and fibronectin. BUMPT cells were transfected with circRNA_33702 plasmid construct or control plasmid before being treated with TGF-β1 or saline for 24 hours. (A) Expression of circRNA_33702 detected by real-time qPCR. (B) Protein expression of collagen I, collagen III, and fibronectin detected by western blotting. (C–E) Densitometric measurement of western blot bands for collagen I (C), collagen III (D), and fibronectin (E). Data are expressed as mean plus or minus S.D. (n = 6). #$P < 0.05$ versus control group. *$P < 0.05$ versus TGF-β1 group.

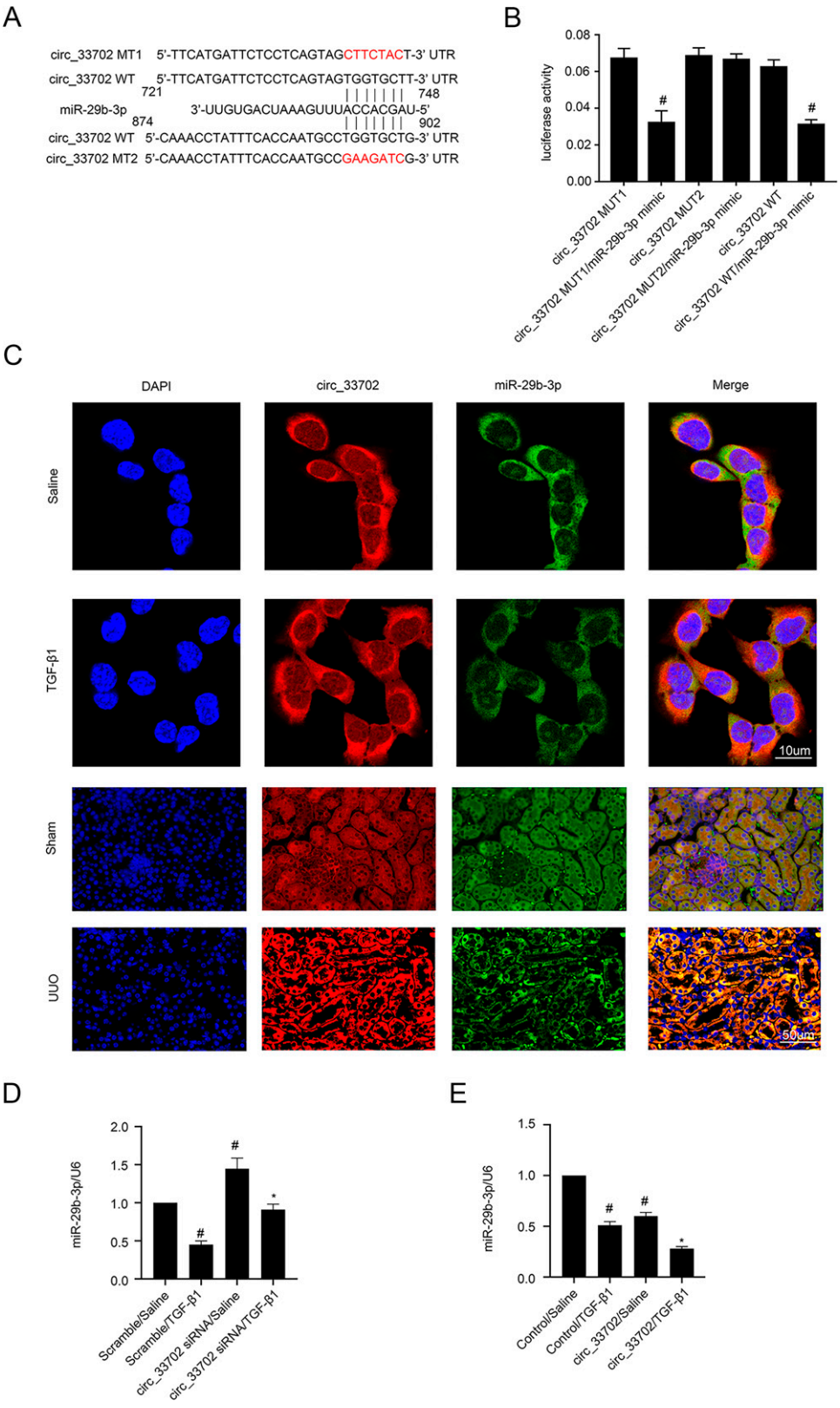

Fig. 4. Negative correlation between circRNA_33702 and miR-29b-3p. (A) Complementary strand of circRNA_33702 to miR-29b-3p predicted by RegRNA 2.0 software. (B) Luciferase activity measurement of cells after cotransfection with circRNA_33702-WT or circRNA_33702-MUTs and miR-29b-3p or scrambled siRNA. (C) Intracellular colocalization of circRNA_33702 and miR-29b-3p in BUMPT cells and in the kidneys of C57BL/6 mice. Scale bar, 10 μm. (D and E) Expression of miR-29b-3p detected by real-time qPCR. Data are expressed as mean plus or minus S.D. (n = 6). #$P < 0.05$ versus scrambled siRNA or control with saline group; *$P < 0.05$, siRNA circRNA_33702 or circRNA_33702 with TGF-β1 group versus scrambled siRNA or control with TGF-β1 group or circRNA_33702 MUT1/miR-29b-3p mimic or circRNA_33702 WT/miR-29b-3p mimic versus other groups.

days 3 and 7 after surgery compared with those from sham controls on days 3 and 7 by circRNA microarray analysis. CircRNA_33702 was one of the most highly expressed circRNA in the kidney tissues and showed a 8.92- and 15.55-fold higher expression in the UUO group on days 3 and 7, respectively, compared with the sham group (Yi et al., 2021). To investigate the expression site of circRNA_33702, BUMPT cells were treated with TGF-β1 before being subjected to fluorescence in situ hybridization analysis. The cell nuclei were stained by DAPI, and 18S rRNA (cytoplasmic positive) and circRNA_33702 were labeled with CY3. As shown in Fig. 1A,

circRNA_33702 was found to be localized in the cytoplasm of BUMPT cells. To evaluate the expression profile of circRNA_33702, real-time qPCR results showed that circRNA_33702 was induced both in TGF-β1–treated BUMPT cells and in UUO mice kidneys (Fig. 1, B and C), indicating that circRNA_33702 may be involved in renal fibrosis. To evaluate the expression of hsa_circ_0026331, homologous with circRNA_33702, real-time qPCR results showed that hsa_circ_0026331 was induced in TGF-β1–treated HK-2 cells (Fig. 1D).

Inhibition of circRNA_33702/hsa_circ_0026331 Expression Attenuated the TGF-β1–Induced Expression of Collagen I, Collagen III, and Fibronectin. Next, we examined the role of circRNA_33702 in TGF-β1–treated BUMPT cells and the homologous hsa_circ_002633 in TGF-β1–treated HK-2 cells. As shown in Fig. 2, A and F, transfection of BUMPT cells with circRNA_33702 siRNA inhibited the TGF-β1–induced expression of circRNA_33702, and transfection of HK-2 cells with hsa_circ_0026331 siRNA inhibited the TGF-β1–induced expression of hsa_circ_0026331. Furthermore, inhibition of circRNA_33702 or hsa_circ_0026331 expression attenuated the expression of collagen I, collagen III, and fibronectin, both at basal levels and TGF-β1–induced levels (Fig. 2, B–E and I–M). These results indicated that inhibition of circRNA_33702 or the homologous hsa_circ_0026331 is capable of relieving TGF-β1–induced expression of collagen I, collagen III, and fibronectin in mouse or human renal tubular epithelial cells, suggesting that circ RNA_33702 with the homologous hsa_circ_002633 may play a role as a profibrosis mediator in renal tubular epithelial cells.

Overexpression of circRNA_33702 Aggravated the TGF-β1–Induced Expression of Collagen I, Collagen III, and Fibronectin. To further explore the effect of circ RNA_33702 on TGF-β1–induced collagen I, collagen III, and fibronectin, BUMPT cells were transfected with circRNA_33702 plasmid constructs. As shown in Fig. 3A, the expression of circRNA_33702 in BUMPT cells was increased after transfection of circRNA_33702. The overexpression of circRNA_33702 enhanced the expression of collagen I, collagen III, and fibronectin, not only at basal levels but also at TGF-β1–induced levels (Fig. 3, B–E). These results further demonstrate the profibrosis function of circRNA_33702 in TGF-β1–treated BUMPT cells.

CircRNA_33702 Binds Directly to miR-29b-3p. Prediction using RegRNA 2.0 software showed that circRNA_33702 exhibits two potential binding sites of miR-29b-3p, indicating that miR-29b-3p may be a potential target of circRNA_33702 (Fig. 4A). Luciferase reporter assays demonstrated that miR-29b-3p mimic could inhibit the luciferase activity of circRNA_33702 WT and circRNA_33702-MUT1, but not circRNA_33702-MUT2, implying that the fragment at base position 741–747 of circRNA_33702 is the real potential binding site of miR-29b-3p (Fig. 4B). Intracellular colocalization analysis showed overlapping signals of circRNA_33702 and miR-29b-3p in the cytoplasm of BUMPT cells and renal tubular cells of C57BL/6 mouse kidneys, indicating that circRNA_33702 and miR-29b-3p may have physical interaction (Fig. 4C). The TGF-β1–suppressed expression of miR-29b-3p was enhanced through knockdown of circRNA_33702, and this effect was reversed through overexpression of circRNA_33702 (Fig. 4, D and E). These results demonstrated that circRNA_33702 can directly interact with miR-29b-3p.

MiR-29b-3p Inhibited TGF-β1–Induced ECM Accumulation in BUMPT Cells. Previous studies have suggested that miR-29b-3p has an antifibrosis role in liver and cardiac fibrosis (Marques et al., 2016; Ni et al., 2019), but the role of miR-29b-3p in renal fibrosis remains unclear. Real-time qPCR confirmed that miR-29b-3p mimic increased the

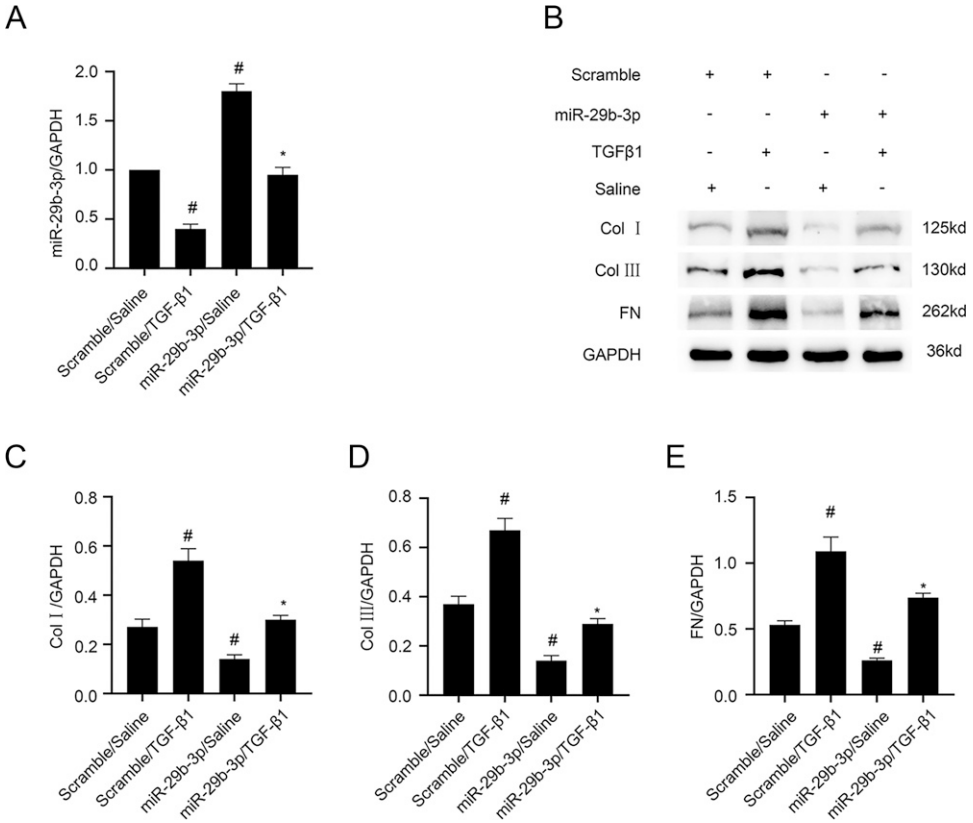

Fig. 5. Overexpression of miR-29b-3p relieved the TGF-β1–induced expression of collagen I, collagen III, and fibronectin. BUMPT cells were transfected with 100 nM miR-29b-3p or scrambled siRNA before being treated with TGF-β1 or saline for 24 hours. (A) Real-time qPCR analysis of miR-29b-3p expression. (B) Western blot analysis of collagen I, collagen III, and fibronectin expression. (C–E) Densitometric measurement of western blot bands for collagen I (C), collagen III (D), and fibronectin (E). Data are expressed as mean plus or minus S.D. (n = 6). #$P < 0.05$ versus scrambled siRNA group. *$P < 0.05$ versus TGF-β1 group.

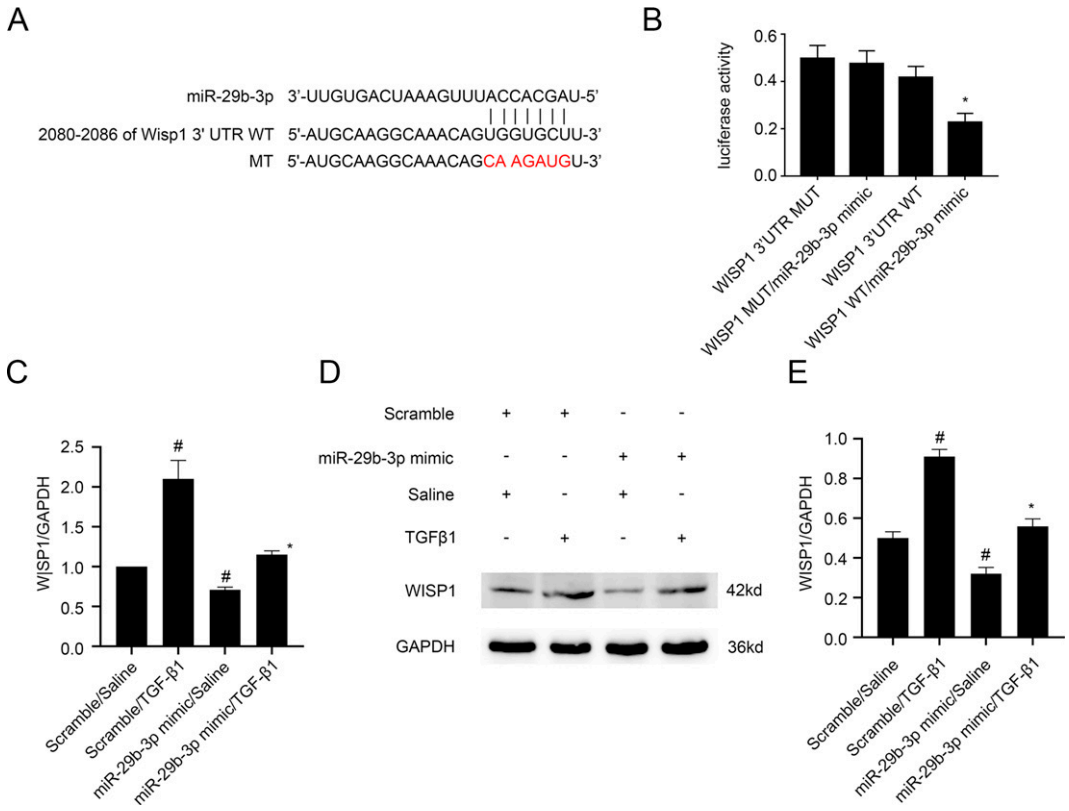

Fig. 6. WISP1 was identified as a target gene of miR-29b-3p. BUMPT cells were transfected with miR-29b-3p analog (100 nM) before being treated with TGF-β1 for 24 hours. (A) MiR-29b-3p complementary binding sites in the 3′UTR of mice WISP1 mRNA. (B) Analysis of luciferase activities in cells after cotransfection with 3′ UTR luciferase reporter vector of mice WT or MUT-WISP1 and miR-29b-3p or miR-NC. (C) Real-time qPCR analysis of WISP1 mRNA expression. (D) Protein expression of WISP1 detected by western blotting. (E) Densitometric measurement of western blot band for WISP1. #$P < 0.05$ versus scrambled siRNA group; *$P < 0.05$, miR-29b-3p analog with TGF-β1 group versus scrambled siRNA with TGF-β1 group or WISP1 WT/miR-29b-3p analog versus other groups.

expression of miR-29b-3p in BUMPT cells (Fig. 5A). Following transfection of BUMPT cells with miR-29b-3p mimic, the TGF-β1–induced expression of collagen I, collagen III, and fibronectin was decreased (Fig. 5, B–E). These results showed that miR-29b-3p inhibits TGF-β1–induced ECM accumulation in BUMPT cells.

WISP1 Is a Target Gene of miR-29b-3p. WISP1 has been suggested to be a mediator of TGF-β1–induced renal fibrosis. As shown in Fig. 6A, WISP1 was predicted by miRbase software as a potential target of miR-29b-3p. Luciferase assay demonstrated that, although miR-29b-3p mimic inhibited the luciferase activity of WISP1-WT, it had no effect on the luciferase activity of WISP1-MUT (Fig. 6B). Furthermore, miR-29b-3p mimic was observed to downregulate the TGF-β1–induced expression of WISP1 (Fig. 6, C–E). Taken together, WISP1 may be a direct target of miR-29b-3p.

MiR-29b-3p Reversed the Profibrotic Effect of circ RNA_33702. Next, we explored whether miR-29b-3p is capable of reversing the effect of circRNA_33702 in BUMPT cells. The transfection efficiency of circRNA_33702 siRNA and miR-29b-3p inhibitor were firstly verified by real-time qPCR (Fig. 7, A and B). Western blot analysis showed that inhibition of circRNA_33702 expression relieved the TGF-β1–induced expression of collagen I, collagen III, fibronectin, and WISP1, whereas miR-29b-3p inhibitor reversed the effect of circRNA_33702 and increased the expression of collagen I, collagen III, fibronectin, and WISP1 (Fig. 7, C–G). These observations indicated that circRNA_33702 may promote renal fibrosis by inhibiting the expression of miR-29b-3p.

Inhibition of circRNA_33702 or WISP1 Attenuated UUO-Induced Renal Fibrosis. To verify our in vitro findings, the expression of circRNA_33702 in male C57BL/6 mice that were on a 7-day UUO treatment was knocked down by injecting circRNA_33702 siRNA on day 1 before surgery and on day 3 after surgery. As shown in Fig. 9A, real-time qPCR indicated that the expression of circRNA_33702 was inhibited, both in UUO mice and in sham control mice, confirming that the knockdown of circRNA_33702 was efficient. The expression of miR-29b-3p that was suppressed in obstructive kidneys was observed to be resumed through the knockdown of circRNA_33702 (Fig. 9B). H&E staining showed that circRNA_33702 was capable of relieving UUO-induced tubular dilation and atrophy in mouse kidneys, and Masson's staining demonstrated that circRNA_33702 was effective in attenuating UUO-induced ECM accumulation (Fig. 8B). Quantitative analysis of fibrotic areas was performed according to the intensities of H&E and Masson's staining (Fig. 8F). Immunohistochemical staining demonstrated that knockdown of circRNA_33702 successfully attenuated the UUO-induced expression of collagen I, collagen III, and fibronectin (Fig. 8, C–E and G). Immunoblotting further verified that the UUO-induced expression of collagen I, collagen III, fibronectin, and WISP1 were relieved through the knockdown of circRNA_33702 (Fig. 9, C–G). As shown in Fig. 9, A and I, immunoblotting indicated that the expression of WISP1 was inhibited, both in UUO mice and in sham control mice, confirming that the knockdown of WISP1 was efficient. The UUO-induced expression of collagen I, collagen III, and fibronectin were relieved through the knockdown of WISP1 (Fig. 9, H–M). Taken together, these data demonstrated that circRNA_33702 may promote renal fibrosis via the miR-29b-3p/WISP1 axis.

Discussion

With an increasing prevalence globally, renal fibrosis is commonly diagnosed in all chronic kidney diseases. Unfortunately,

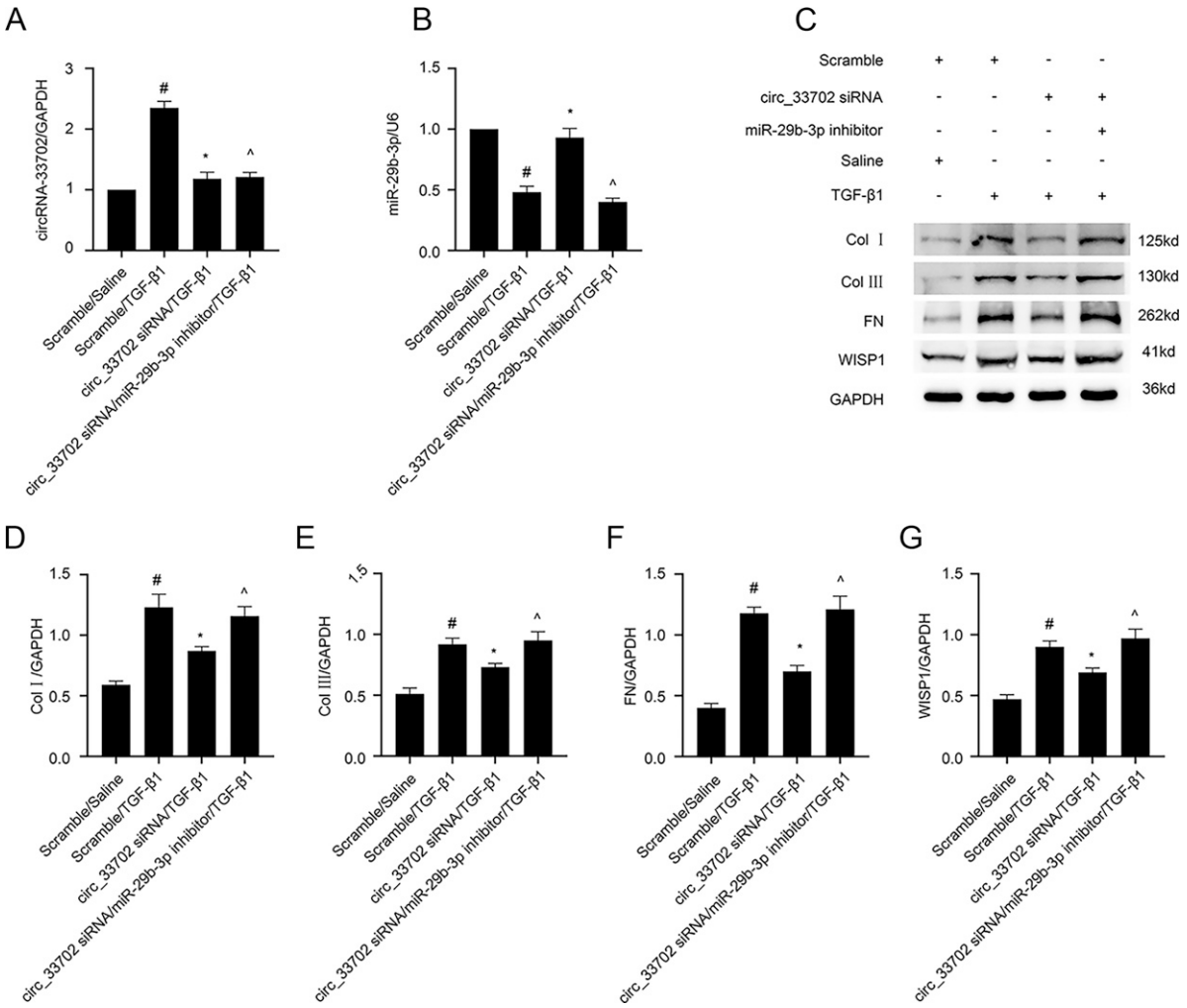

Fig. 7. CircRNA_33702 siRNA relieved TGF-β1–induced ECM accumulation, which can be reversed by miR-29b-3p inhibitor. BUMPT cells were cotransfected with circRNA_33702 siRNA and miR-29b-3p inhibitor or scrambled siRNA before being treated with TGF-β1 for 24 hours. (A) Expression of circRNA_33702 detected by real-time qPCR. (B) Expression of miR-29b-3p detected by real-time qPCR. (C) Protein expression of collagen I, collagen III, fibronectin, and WISP1 detected by western blotting. (D–G) Densitometric measurement of western blot bands for collagen I (D), collagen III (E), fibronectin (F), and WISP1 (G). Data are expressed as mean plus or minus S.D. (n = 6). #$P < 0.05$, scrambled siRNA with TGF-β1 group versus scramble group; *$P < 0.05$, circRNA_33702 siRNA with TGF-β1 group versus scrambled siRNA with TGF-β1 group; ^$P < 0.05$, circRNA_33702 siRNA plus miR-29b-3p inhibitor with TGF-β1 group versus circRNA_33702 siRNA with TGF-β1 group.

there are very few available therapeutic options. For the first time, this study identified the role of circRNA_33702 in TGF-β1–treated BUMPT cells and in the obstructive kidneys of mice and the role of the homologous hsa_circ_0026331 in TGF-β1–treated HK-2 cells. Although the expression of circRNA_33702 was found to be enhanced in renal fibrosis, overexpression of circRNA_33702 was observed to aggravate TGF-β1–induced collagen I, collagen III, and fibronectin. Conversely, knockdown of circRNA_33702 with the homologous hsa_circ_0026331 was shown to attenuate TGF-β1–induced collagen I, collagen III, and fibronectin. In terms of regulatory mechanism, our results suggest that the expression of miR-29b-3p is negatively regulated by circRNA_33702 and that WISP1 is a target gene of miR-29b-3p. Moreover, renal fibrosis was found to be attenuated through the inhibition of circRNA_33702 in mice UUO model. Our study provides direct evidence that demonstrates the association between the circRNA_33702/miR-29b-3p/WISP1 axis and renal fibrosis. The findings in this study may facilitate the development of therapeutic interventions for kidney fibrosis (Fig. 10).

An increasing number of studies have demonstrated that circRNAs are involved in renal diseases. Xiong et al. (2019) have found that the expression of circRNA_ZNF609 is upregulated in renal cell carcinoma and that the overexpression of circRNA_ZNF609 promotes cell proliferation and invasion via the miR-138-5p/FOXP4 axis. Additionally, Deng et al. (2019) have demonstrated that circRNA_ANRIL can promote lipopolysaccharide-induced inflammation and apoptosis of HK2 cells. However, there have been very few studies that focus on the effect of circRNA in renal fibrosis. In this study, we found that the expression of circRNA_33702 was upregulated in TGF-β1–treated BUMPT cells as well as in UUO mice. In addition, although circRNA_33702 knockdown was found to aggravate the TGF-β1–induced collagen I, collagen III, and fibronectin, the observed effect was successfully reversed though the overexpression of circRNA_33702. Our data suggest that circRNA_33702 plays a profibrotic role in TGF-β1–treated BUMPT cells.

An increasing number of studies have demonstrated that circRNAs, a new category of endogenous noncoding RNA, can decrease miRNA abundance by sponging miRNA to regulate

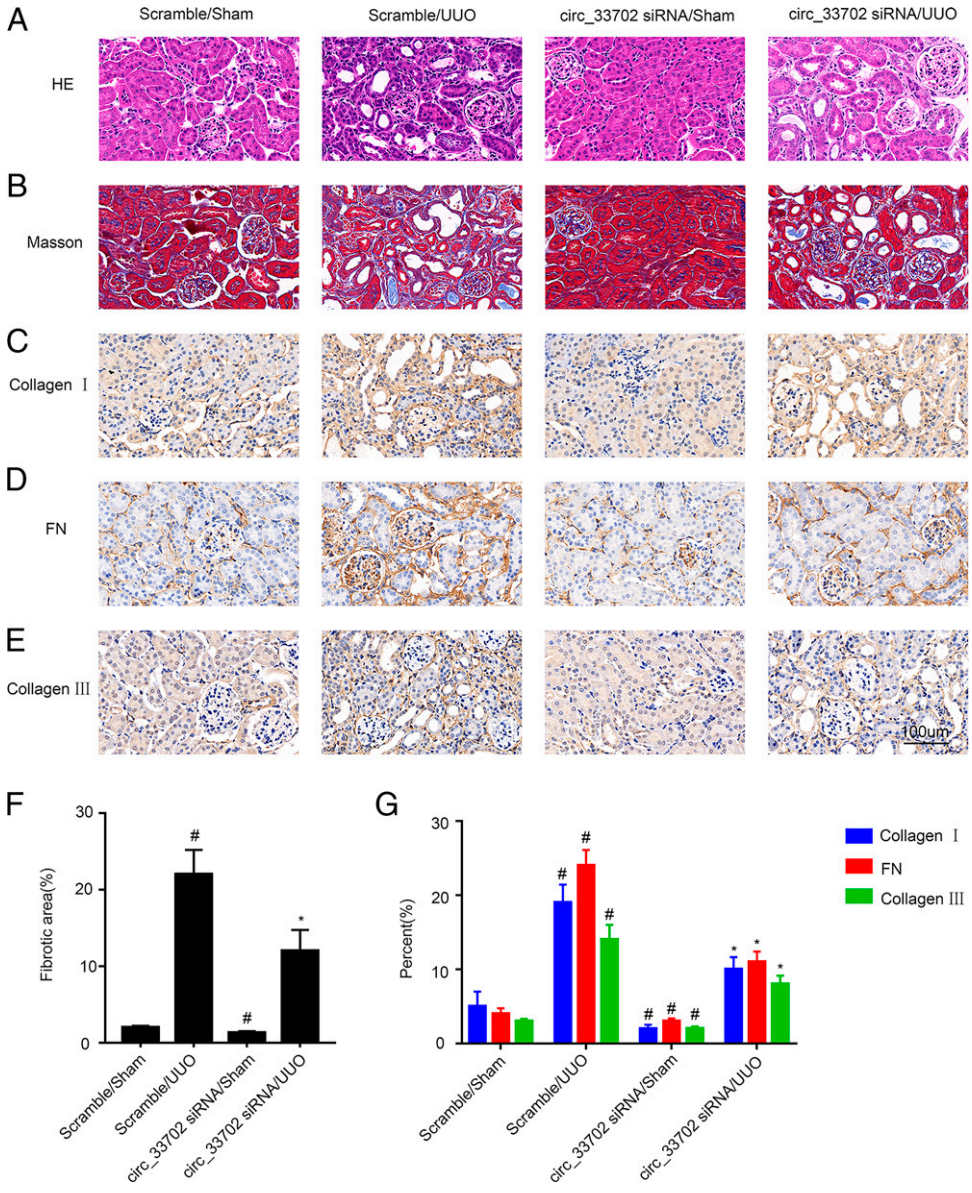

Fig. 8. Inhibition of circRNA_33702 attenuated UUO-induced renal fibrosis. The left ureter of male C57BL/6 mice was ligated to establish the UUO model for 7 days. (A) Renal tissues stained with H&E. (B) Renal tissues stained with Masson's trichrome. (C–E) Immunohistochemistry of collagen I, collagen III, and fibronectin. Scale bar, 100 μm. (F) Quantify tubulointerstitial fibrosis in the kidney cortex. (G) Quantification of immunohistochemistry staining. Data are expressed as mean plus or minus S.D. (n = 6). #$P < 0.05$ versus sham group. *$P < 0.05$ versus scrambled siRNA with UUO group. Original magnification, ×200.

targeted gene expression. In this study, through dual-luciferase reporter assay, circRNA_33702 was demonstrated to be capable of binding miR-29b-3p directly. In addition, through fluorescence in situ hybridization colocalization assay, circRNA_33702 was revealed to interact with miR-29b-3p, both in BUMPT cells and in mouse kidneys. Moreover, miR-29b-3p inhibitor was found to successfully reverse the effect of circRNA_33702 knockdown and subsequently promote ECM accumulation. The observations above demonstrate that miR-29b-3p is a direct target of circRNA_33702.

Many studies have shown that miR-29b-3p is involved in fibrosis. Ni et al. (2019) have reported that miR-29b-3p, as a direct target of circRNA-HIPK3, can inhibit the proliferation and migration of cardiac fibroblasts and that the inhibition effect can be altered by targeting α-SMA, COL1A1, and COL3A1. Yang et al. (2017) have found that miR-29b-3p can prevent granulomatous liver fibrosis through direct inhibition of COL1A1 and COL3A1. Zhang et al. (2018) have demonstrated that carnosic acid can alleviate bile duct ligation–induced liver fibrosis in rats by modulating the miR-29b-3p/HMGB1/TLR4/NF-κB signaling pathway. Our study revealed that overexpression of miR-29b-3p can inhibit the TGF-β1–induced ECM accumulation in BUMPT cells and that WISP1 is a potential target of miR-29b-3p. Furthermore, we demonstrated that miR-29b-3p interacts directly with WISP1 and that miR-29b-3p overexpression can suppress TGF-β1–induced WISP1 expression. Taken together, these results show that WISP1 is a target of miR-29b-3p.

Several studies have shown that WISP1 is involved in the fibrosis of various organs, including the kidney. Yang et al. (2020b) have explored the functional role and mechanism of WISP1 in renal fibrosis using TGF-β1–treated tubular epithelial cells and UUO mouse models; they have found that WISP1 can upregulate the expression of collagen I, FN, and α-SMA, indicating that WISP1 can promote renal fibrosis by inducing autophagy. Chen et al. (2019) have reported that knockdown of WISP1 can suppress the activation of the Wnt/β-actin catenin signaling pathway, which then decreases the Epithelial-

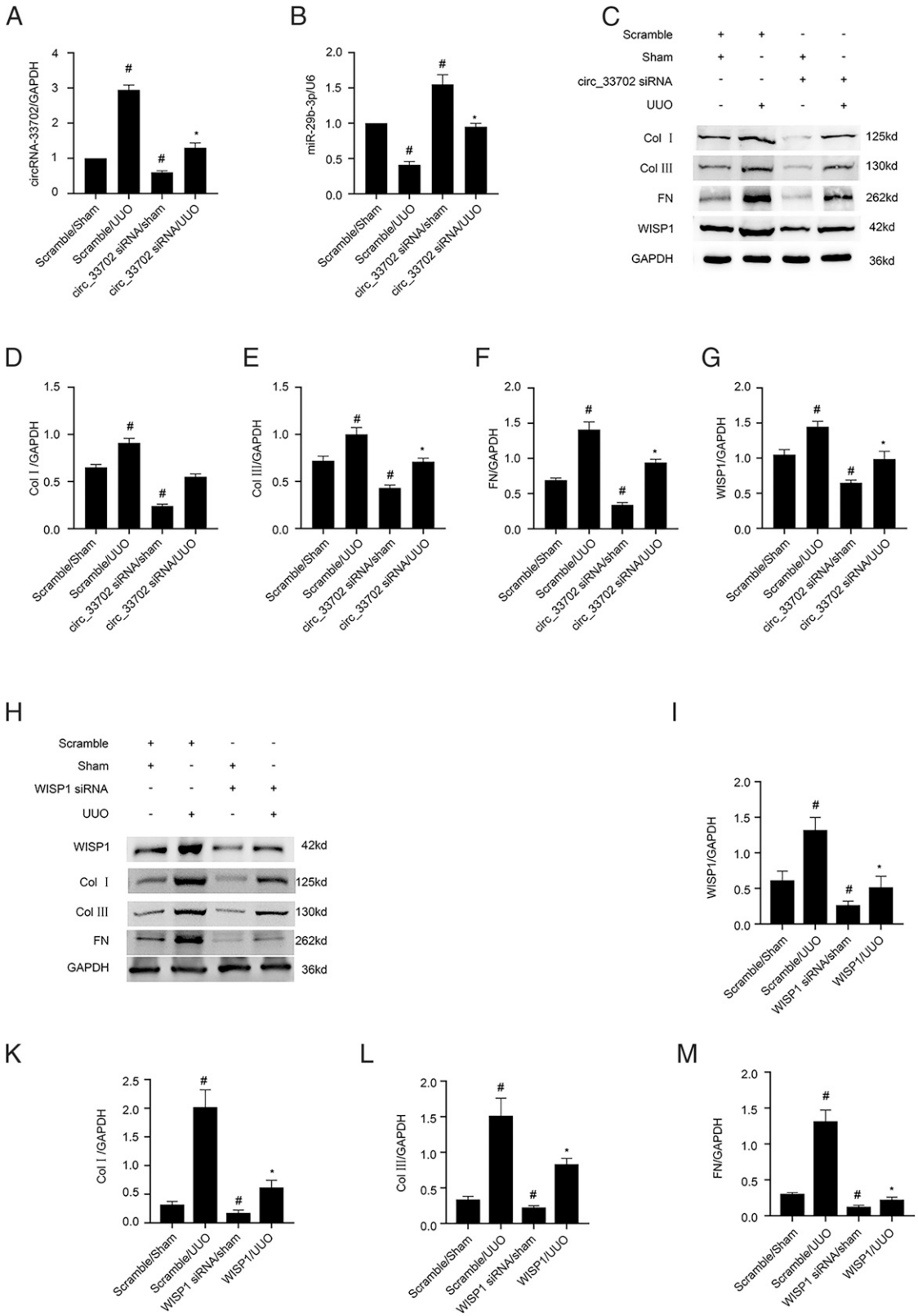

Fig. 9. Inhibition of circRNA_33702 or WISP1 attenuated the UUO-induced expression of collagen I, collagen III, and fibronectin. The left ureter of male C57BL/6 mice was ligated to establish the UUO model for 7 days. (A) Real-time qPCR analysis of circRNA_33702. (B) Real-time qPCR analysis of miR-29b-3p. (C) Protein expression of collagen I, collagen III, fibronectin, and WISP1 detected by western blotting. (D–G) Densitometric measurement of western blot bands for collagen I (D), collagen III (E), fibronectin (F) and WISP1(G). (H) Protein expression of collagen I, collagen III, fibronectin, and WISP1 detected by western blotting. (I–M) Densitometric measurement of western blot bands for WISP1 (I), collagen I (K), collagen III (L), and fibronectin (M). #$P < 0.05$ versus sham group. *$P < 0.05$ versus scrambled siRNA with UUO group.

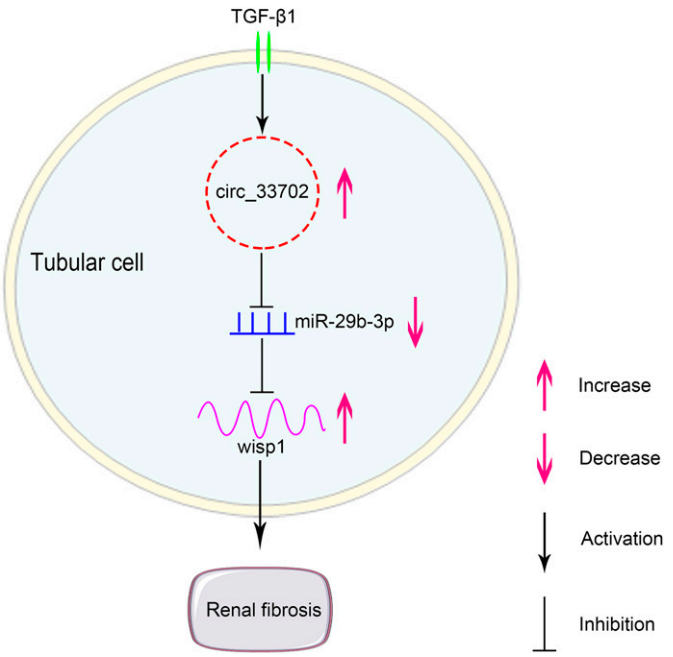

Fig. 10. Molecular mechanism of circRNA_33702 in TGF-β1–induced renal fibrosis. The expression of circRNA_33702 was induced in TGF-β1–treated BUMPT cells and in UUO mouse kidneys. CircRNA_33702 sponges miR-29b-3p to upregulate the expression of WISP1, which then promotes renal fibrosis.

Mesenchymal Transition (EMT) of renal tubular epithelial cells (TECs) in uremic rats. In this study, we demonstrated that knockdown of circRNA_33702 can relieve TGF-β1–induced renal fibrosis through the downregulation of WISP1 and that the observed effect can be reversed by miR-29b-3p inhibitor. Our in vitro observations were confirmed using UUO mouse kidney samples by showing that the inhibition of circRNA_33702 can attenuate renal fibrosis in UUO mice by targeting the miR-29b-3p/WISP1 axis.

In summary, our work demonstrated that the expression of circRNA_33702 is induced in renal fibrosis. In addition, overexpression of circRNA_33702 was found to aggravate TGF-β1–induced collagen I, collagen III, and fibronectin, whereas knockdown of circRNA_33702 and the homologous hsa_circ_0026331 was observed to relieve TGF-β1–induced collagen I, collagen III, and fibronectin. Furthermore, we showed that overexpressed circRNA_33702 directly interacts with miR-29b-3p to upregulate WISP1 expression, which ultimately promotes renal fibrosis. Our findings suggested that circRNA_33702 plays a profibrosis role and that circRNA_33702 and the homologous hsa_circ_0026331 may be novel therapeutic targets of renal fibrosis.

Authorship Contributions

Participated in research design: Wang, Li.
Conducted experiments: Ai, Yi.
Contributed new reagents or analytic tools: Wang.
Performed data analysis: Ai, Yi.
Wrote or contributed to the writing of the manuscript: Ai, Yi, Li.

References

Böttinger EP and Bitzer M (2002) TGF-beta signaling in renal disease. *J Am Soc Nephrol* **13**:2600–2610.
Chen Y-Z, Sun D-Q, Zheng Y, Zheng G-K, Chen R-Q, Lin M, Huang L-F, Huang C, Song D, and Wu B-Q (2019) WISP1 silencing confers protection against epithelial-mesenchymal transition of renal tubular epithelial cells in rats via inactivation of the wnt/β-catenin signaling pathway in uremia. *J Cell Physiol* **234**:9673–9686.
Chevalier RL, Forbes MS, and Thornhill BA (2009) Ureteral obstruction as a model of renal interstitial fibrosis and obstructive nephropathy. *Kidney Int* **75**:1145–1152.
Cui S and Zhang L (2020) circ_001653 Silencing Promotes the Proliferation and ECM Synthesis of NPCs in IDD by Downregulating miR-486-3p-Mediated CEMIP. *Mol Ther Nucleic Acids* **20**:385–399.
Deng W, Chen K, Liu S, and Wang Y (2019) Silencing circular ANRIL protects HK-2 cells from lipopolysaccharide-induced inflammatory injury through up-regulating microRNA-9. *Artif Cells Nanomed Biotechnol* **47**:3478–3484. [Expression of concern published in *Artif Cells Nanomed Biotechnol* (2021) **49**:283].
Eddy AA (2014) Overview of the cellular and molecular basis of kidney fibrosis. *Kidney Int Suppl* **4**:2–8.
Guo JU, Agarwal V, Guo H, and Bartel DP (2014) Expanded identification and characterization of mammalian circular RNAs. *Genome Biol* **15**:409.
Haque S and Harries LW (2017) Circular RNAs (circRNAs) in Health and Disease. *Genes (Basel)* **8**:353.
Hu W, Han Q, Zhao L, and Wang L (2019) Circular RNA circRNA_15698 aggravates the extracellular matrix of diabetic nephropathy mesangial cells via miR-185/TGF-β1. *J Cell Physiol* **234**:1469–1476.
Kong P, Yu Y, Wang L, Dou YQ, Zhang XH, Cui Y, Wang HY, Yong YT, Liu YB, Hu HJ, et al. (2019) circ-Sirt1 controls NF-κB activation via sequence-specific interaction and enhancement of SIRT1 expression by binding to miR-132/212 in vascular smooth muscle cells. *Nucleic Acids Res* **47**:3580–3593.
Liu Y (2011) Cellular and molecular mechanisms of renal fibrosis. *Nat Rev Nephrol* **7**:684–696.
Luan J, Jiao C, Kong W, Fu J, Qu W, Chen Y, Zhu X, Zeng Y, Guo G, Qi H, et al. (2018) circHLA-C Plays an Important Role in Lupus Nephritis by Sponging miR-150. *Mol Ther Nucleic Acids* **10**:245–253.
Marques FZ, Vizi D, Khammy O, Mariani JA, and Kaye DM (2016) The transcardiac gradient of cardio-microRNAs in the failing heart. *Eur J Heart Fail* **18**:1000–1008.
Ni H, Li W, Zhuge Y, Xu S, Wang Y, Chen Y, Shen G, and Wang F (2019) Inhibition of circHIPK3 prevents angiotensin II-induced cardiac fibrosis by sponging miR-29b-3p. *Int J Cardiol* **292**:188–196.
Peng J, Li X, Zhang D, Chen J-K, Su Y, Smith SB, and Dong Z (2015) Hyperglycemia, p53, and mitochondrial pathway of apoptosis are involved in the susceptibility of diabetic models to ischemic acute kidney injury. *Kidney Int* **87**:137–150.
Qi R and Yang C (2018) Renal tubular epithelial cells: the neglected mediator of tubulointerstitial fibrosis after injury. *Cell Death Dis* **9**:1126.
Song Y-Z and Li J-F (2018) Circular RNA hsa_circ_0001564 regulates osteosarcoma proliferation and apoptosis by acting miRNA sponge. *Biochem Biophys Res Commun* **495**:2369–2375.
Wang J, Li H, Qiu S, Dong Z, Xiang X, and Zhang D (2017) MBD2 upregulates miR-301a-5p to induce kidney cell apoptosis during vancomycin-induced AKI. *Cell Death Dis* **8**:e3120.
Xiong Y, Zhang J, and Song C (2019) CircRNA ZNF609 functions as a competitive endogenous RNA to regulate FOXP4 expression by sponging miR-138-5p in renal carcinoma. *J Cell Physiol* **234**:10646–10654.
Xu L, Li X, Zhang F, Wu L, Dong Z, and Zhang D (2019) EGFR drives the progression of AKI to CKD through HIPK2 overexpression. *Theranostics* **9**:2712–2726.
Yang L, Liang H, Meng X, Shen L, Guan Z, Hei B, Yu H, Qi S, and Wen X (2020a) mmu_circ_0000790 Is Involved in Pulmonary Vascular Remodeling in Mice with HPH via MicroRNA-374c-Mediated FOXC1. *Mol Ther Nucleic Acids* **20**:292–307.
Yang R, Xu X, Li H, Chen J, Xiang X, Dong Z, and Zhang D (2017) p53 induces miR199a-3p to suppress SOCS7 for STAT3 activation and renal fibrosis in UUO. *Sci Rep* **7**:43409.
Yang X, Wang H, Tu Y, Li Y, Zou Y, Li G, Wang L, and Zhong X (2020b) WNT1-inducible signaling protein-1 mediates TGF-β1-induced renal fibrosis in tubular epithelial cells and unilateral ureteral obstruction mouse models via autophagy. *J Cell Physiol* **235**:2009–2022.
Yi L, Ai K, Li H, Qiu S, Li Y, Wang Y, Li X, Zheng P, Chen J, Wu D, et al. (2021) CircRNA_30032 promotes renal fibrosis in UUO model mice via miRNA-96-5p/HBEGF/KRAS axis. *Aging (Albany NY)* **13**:12780–12799.
Zeisberg M and Neilson EG (2010) Mechanisms of tubulointerstitial fibrosis. *J Am Soc Nephrol* **21**:1819–1834.
Zhang P, Yi L, Qu S, Dai J, Li X, Liu B, Li H, Ai K, Zheng P, Qiu S, et al. (2020) The Biomarker TCONS_00016233 Drives Septic AKI by Targeting the miR-22-3p/AIFM1 Signaling Axis. *Mol Ther Nucleic Acids* **19**:1027–1042.
Zhang S, Wang Z, Zhu J, Xu T, Zhao Y, Zhao H, Tang F, Li Z, Zhou J, Gao D, et al. (2018) Carnosic Acid Alleviates BDL-Induced Liver Fibrosis through miR-29b-3p-Mediated Inhibition of the High-Mobility Group Box 1/Toll-Like Receptor 4 Signaling Pathway in Rats. *Front Pharmacol* **8**:976.
Zhong X, Tu YJ, Li Y, Zhang P, Wang W, Chen SS, Li L, Chung AC, Lan HY, Chen HY, et al. (2017) Serum levels of WNT1-inducible signaling pathway protein-1 (WISP-1): a noninvasive biomarker of renal fibrosis in subjects with chronic kidney disease. *Am J Transl Res* **9**:2920–2932.
Zhong Y, Du Y, Yang X, Mo Y, Fan C, Xiong F, Ren D, Ye X, Li C, Wang Y, et al. (2018) Circular RNAs function as ceRNAs to regulate and control human cancer progression. *Mol Cancer* **17**:79.
Zhou B, Zheng P, Li Z, Li H, Wang X, Shi Z, and Han Q (2018) CircPCNXL2 sponges miR-153 to promote the proliferation and invasion of renal cancer cells through upregulating ZEB2. *Cell Cycle* **17**:2644–2654.

Address correspondence to: Dr. Yinhuai Wang. E-mail: wangyinhuai@csu.edu.cn; or Dr. Yuan Li. E-mail: yuanlixy@csu.edu.cn